



## Exploring Indolyl Triazoles: Synthesis, Computational Profiling and Antimicrobial Assessment

GEETHA BIRUDALA<sup>1,✉</sup>, RAJENDRA DNYANDEO DIGHE<sup>2,✉</sup>, SARAVANAKUMAR KASIMEDU<sup>3,✉</sup>,  
SOWJANYA PULIPATI<sup>4,✉</sup>, HARI VELURU<sup>5,✉</sup>, NAVEENKUMAR GANDUPALLY<sup>6,✉</sup> and GURINDERDEEP SINGH<sup>7,✉</sup>

<sup>1</sup>Faculty of Pharmacy, Dr. M.G.R. Educational and Research Institute, Velappanchavadi, Chennai-600077, India

<sup>2</sup>Department of Pharmaceutical Chemistry, K.B.H.S.S. Trust's Institute of Pharmacy, Malegaon, Nashik-423105, India

<sup>3</sup>Department of Pharmaceutics, Seven Hills College of Pharmacy, Venkatramapuram, Tirupati-517561, India

<sup>4</sup>Department of Pharmaceutics, Vignan Pharmacy College, Vadlamudi-522213, India

<sup>5</sup>MB School of Pharmaceutical Sciences (Erstwhile Sree Vidyanikethan College of Pharmacy), Mohan Babu University, Sree Sainath Nagar, A. Rangampeta, Tirupati-517102, India

<sup>6</sup>Department of Pharmacology, Sri Venkateswara College of Pharmacy, RVS Nagar, Chittoor-517127, India

<sup>7</sup>Department of Pharmaceutical Sciences and Drug Research, Punjabi University, Patiala-147002, India

\*Corresponding author: E-mail: [gdspharma4@gmail.com](mailto:gdspharma4@gmail.com)

Received: 18 June 2024;

Accepted: 3 August 2024;

Published online: 30 August 2024;

AJC-21741

In this work, a series of new indolyl-triazole compounds (**IT1-8**) were synthesized, characterized and evaluated for their *in vitro* antimicrobial activities. The synthesis involved reactions of indole acetic acid and hydrazine, followed by cyclization with various reagents, yielding triazole compounds elucidated by TLC, IR, NMR, and mass spectral data. Computational profiling using PASS and Molinspiration indicated potential antitubercular and anticancer activities, with compounds **IT1** and **IT2** showing high bioactivity scores. ProTox 3.0 analysis identified compound **IT5** as the safest compound regarding toxicity. The synthesized indolyl-triazoles exhibited significant antimicrobial activity, especially against *Mycobacterium tuberculosis* and various bacterial strains. The experimental assessments revealed unexpected antibacterial activities, particularly in compounds **IT5** and **IT6**, highlighting the significance of halogenated phenyl rings and indolyl moieties in their efficacy. The study underscores the potential of indolyl-triazoles as antimicrobial agents and the role of computational tools in drug discovery, while also noting the discrepancy between *in silico* predictions and experimental results, suggesting the need for further exploration of structure-activity relationships (SAR).

**Keywords:** Indolyl triazoles, Synthesis, *In silico* profiling, Antitubercular activity, Antibacterial activity.

### INTRODUCTION

Antimicrobial resistance (AMR) poses a critical global health challenge, worsened by the widespread overuse and misuse of antibiotics during the COVID-19 pandemic. The World Health Organization (WHO) reports alarmingly high rates of antibiotic usage, especially among patients with severe or critical COVID-19, reaching an average of 81% globally. This excessive antibiotic consumption not only fails to address viral infections but also fuels the development of drug-resistant bacterial strains, contributing to the silent spread of AMR [1-3].

The consequences of antimicrobial resistance (AMR) are significant, as evidenced by the fact that in 2019 alone, around 1.27 million individuals worldwide lost their lives as a result

of bacterial resistance, which led to an additional 4.95 million fatalities owing to complications associated with AMR [4]. Beyond the terrible impact it has on human health, AMR also imposes major economic implications. The World Bank forecasts additional healthcare expenses of 1 trillion US\$ by 2050 and annual global GDP declines ranging from 1 to 3.4 trillion US\$ by 2030 [5].

The escalation of multidrug-resistant tuberculosis (MDR-TB) has made tuberculosis (TB) a major contributor to AMR. MDR-TB presents formidable challenges due to the toxicity and high cost of second-line treatments, which can inadvertently lead to further drug resistance. This scenario underscores MDR-TB as a pressing public health crisis, compounded by the fact that only 40% of affected patients receive the necessary treat-

ment [6]. According, the latest GLASS report for 2022 shows concerning patterns in the resistance of common infectious bacteria. Significantly, the median reported rates of resistance range from 35-40% for  $\beta$ -lactam-resistant pathogens such as *S. aureus* and *E. coli* across 76 countries. Additionally, a 20% of *E. coli* related urinary tract infections exhibited decreased susceptibility to commonly used antibiotics, highlighting the growing challenge in managing common infections [7].

In response to the urgent need for novel antimicrobial agents, heterocyclic compounds containing nitrogen as a heteroatom have garnered considerable attention [8]. Triazoles, including 1,2,4-triazoles and indoles represent promising scaffolds for drug discovery due to their diverse biological activities, low toxicity profiles and favourable pharmacokinetics. Notably, commercially available drugs such as fluconazole, itraconazole, posaconazole, voriconazole and ribavirin are based on 1,2,4-triazole cores, underscoring their clinical relevance in infectious disease treatment [9,10].

The indole framework, renowned for its pharmacological versatility, has emerged as a vital tool in antimicrobial drug discovery. Researchers have produced drugs targeting critical enzymes in microbial pathways using indole's peculiar structure, demonstrating its vast use in fighting infectious illnesses [11-13]. Among the most intriguing developments in this arena are indolyl triazoles, a class of compounds exhibiting diverse biological activities, including potent antimicrobial properties [14-18]. Previous studies have demonstrated the antimicrobial and antitubercular activity of indolyl triazole hybrids, suggesting their potential as novel therapeutic agents [19,20]. In this context, our research aims to synthesize and evaluate a series of indolyl triazoles using computational approaches to predict their molecular interactions and physico-chemical properties. By combining synthetic chemistry with computational insights, this study seeks to advance innovative antimicrobial solutions in the battle against AMR. The synthesis and evaluation of indolyl triazoles represent a promising approach to address the urgent need for effective and sustainable antimicrobial therapies.

## EXPERIMENTAL

Reagents and solvents were procured from different reputed chemical companies like Sigma Aldrich, Loba Chemicals and Merck and used without purification. Melting points were determined using the open capillary method and are uncorrected. Using Thin layer chromatography (TLC) on silica gel, the progress of the reactions were monitored under UV light. Spectral analyses were conducted with FT-IR on a Shimadzu FT-IR 4000;  $^1\text{H}$  NMR on a Bruker 500 MHz FT NMR and  $^{13}\text{C}$  NMR on a JEOL ECZ 400S spectrometer instruments. The mass spectra were obtained using a JEOL GC mate II GC-Mass spectrometer, operating at 70 electron volts (eV) with the direct insertion probe technique.

**Synthesis of indolyl acetohydrazide:** Indolyl acetohydrazide was synthesized by refluxing a mixture of 10 g of indole-3-acetic acid and 10 g of hydrazine hydrate at 60 °C for 8 h. The advancement of the reaction was tracked by thin layer chromatography (TLC) with a solvent system of 1:1 ethyl

acetate and *n*-hexane. The indolyl acetohydrazide was obtained by filtration and washing the solid product with *n*-hexane.

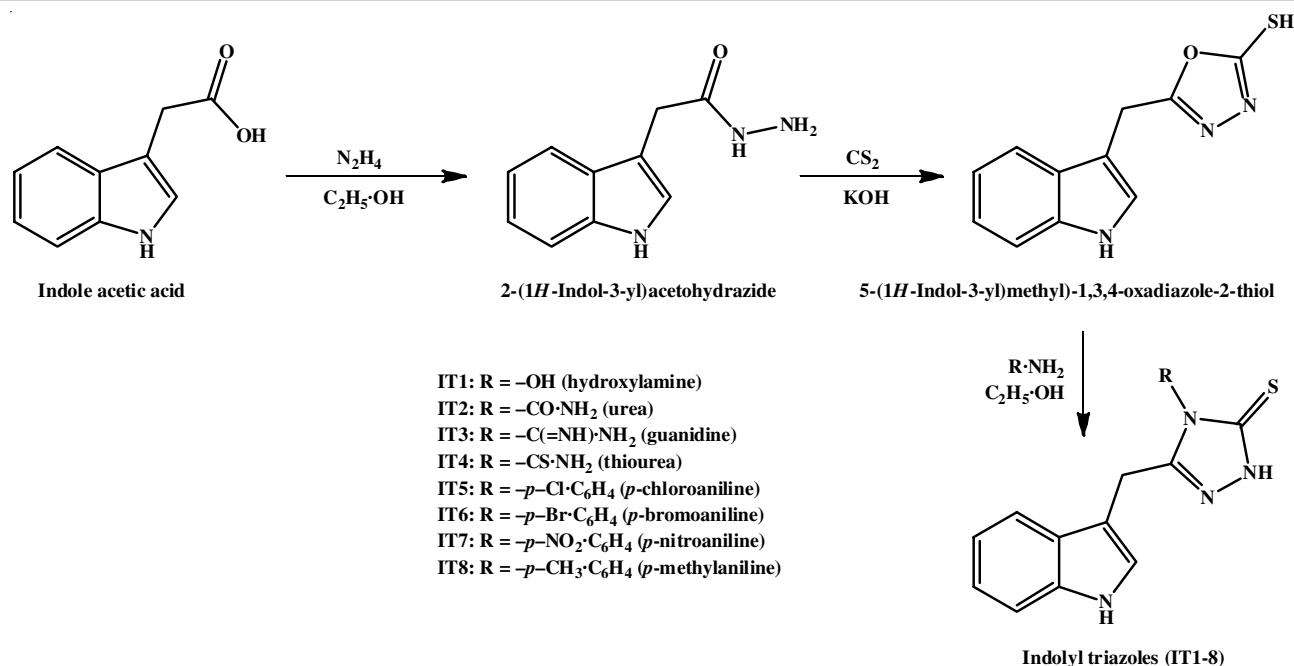
**Synthesis of indolyl oxadiazolothiol intermediate:** Addition of 3 g of carbon disulfide to a mixture of 8 g of indolyl acetohydrazide in 95% ethanol and refluxing for 6 h in basic conditions with KOH produced 5-((1*H*-indol-3-yl)methyl)-1,3,4-oxadiazole-2-thiol. The reaction was monitored by TLC in an ethyl acetate:methanol (3:1) solvent system until only one spot was visible. After the reaction mixture cooled to room temperature, conc. HCl was used to adjust the pH. Then, the reaction mixture was filtrated and then purified with methanol to extract the indolyl oxadiazole thiol intermediate.

**Synthesis of 5-((1*H*-indol-3-yl) methyl)-4-substituted-4*H*-1,2,4-triazole-3-thiones (IT1-8):** In this synthesis, eight alternative reagents with comparable reactivity to hydrazine hydrate were used instead. The reaction of indolyl oxadiazole thiol intermediate and each equivalent reagent of hydrazine hydrate in ethanol was refluxed for a continuous period of 8 h. The advancement of the reaction was monitored by TLC using a mixture of ethyl acetate and *n*-hexane at a 1:1 ratio as solvent system. After the completion of reaction, the obtained precipitates were filtered and rinsed with *n*-hexane to separate the desired products IT1-8 (Scheme-I).

**4-Hydroxy-5-((1*H*-indol-3-yl)methyl)-2,4-dihydro-3*H*-1,2,4-triazole-3-thione (IT1):** Yield: 74%; m.p.: 157-159 °C; FT-IR (KBr,  $\nu_{\text{max}}$ ,  $\text{cm}^{-1}$ ): 3488 (N-H), 3102 (OH), 1588 (C=N), 1524 (C=C), 1439 (C=S);  $^1\text{H}$  NMR (DMSO- $d_6$ ,  $\delta$  ppm): 3.80 (2H, s), 6.91-7.16 (2H, 6.98 (dd), 7.8 (dd), 7.08 (dd)), 7.27-7.46 (2H, 7.34 (dd), 7.41 (tt)), 7.63 (1H, dd);  $^{13}\text{C}$  NMR (DMSO,  $\delta$  ppm): 29.2 (1C, s), 110.5 (1C, s), 111.3 (1C, s), 118.7 (1C, s), 123.2 (1C, s), 127.3 (1C, s), 128.2 (1C, s), 128.4 (1C, s), 136.4 (1C, s), 150.9 (1C, s), 177.4 (1C, s); MS ( $m/z$ , %): 246.05 ( $M^+$ ); Anal. calcd. (found) % for  $\text{C}_{11}\text{H}_{10}\text{N}_4\text{OS}$ : C, 53.64 (53.61); H, 4.09 (4.11); N, 22.75 (22.74); O, 6.50 (6.52); S, 13.02 (13.04).

**3-((1*H*-Indol-3-yl)methyl)-5-thioxo-1,5-dihydro-4*H*-1,2,4-triazole-4-carboxamide (IT2):** Yield: 72%; m.p.: 152-154 °C; FT-IR (KBr,  $\nu_{\text{max}}$ ,  $\text{cm}^{-1}$ ): 3472 (N-H), 1722 (C=O), 1600 (C=N), 1542 (C=C), 1420 (C=S);  $^1\text{H}$  NMR (DMSO- $d_6$ ,  $\delta$  ppm): 3.79 (2H, s), 6.91-7.16 (2H, 6.98 (dd), 7.08 (dd)), 7.27-7.46 (2H, 7.34 (dd), 7.41 (tt)), 7.63 (1H, (dd));  $^{13}\text{C}$  NMR (DMSO,  $\delta$  ppm): 29.2 (1C, s), 110.5 (1C, s), 111.3 (1C, s), 118.7 (1C, s), 123.2 (1C, s), 127.3 (1C, s), 128.2 (1C, s), 128.4 (1C, s), 136.4 (1C, s), 150.9 (1C, s), 152.9 (1C, s), 170.1 (1C, s); MS ( $m/z$ , %): 273.08 ( $M^+$ ); Anal. calcd. (found) % for  $\text{C}_{12}\text{H}_{11}\text{N}_5\text{OS}$ : C, 52.73 (52.76); H, 4.06 (4.02); N, 25.62 (25.64); O, 5.85 (5.88); S, 11.73 (11.71).

**3-((1*H*-Indol-3-yl)methyl)-5-thioxo-1,5-dihydro-4*H*-1,2,4-triazole-4-carboximidamide (IT3):** Yield: 68%; m.p.: 168-170 °C; FT-IR (KBr,  $\nu_{\text{max}}$ ,  $\text{cm}^{-1}$ ): 3489 (N-H), 1592 (C=N), 1581 (C=C), 1422 (C=S);  $^1\text{H}$  NMR (DMSO- $d_6$ ,  $\delta$  ppm): 3.80 (2H, s), 6.91-7.16 (2H, 6.99 (dd), 7.08 (dd)), 7.27-7.45 (2H, 7.34 (dd), 7.40 (tt)), 7.63 (1H, (dd));  $^{13}\text{C}$  NMR (DMSO,  $\delta$  ppm): 29.2 (1C, s), 110.5 (1C, s), 111.3 (1C, s), 118.7 (1C, s), 123.2 (1C, s), 127.3 (1C, s), 128.2 (1C, s), 128.4 (1C, s), 136.4 (1C, s), 150.9 (1C, s), 155.8 (1C, s), 170.1 (1C, s); MS ( $m/z$ , %): 272.02 ( $M^+$ ); Anal. calcd. (found) % for  $\text{C}_{12}\text{H}_{12}\text{N}_6\text{S}$ : C, 52.92 (52.91); H, 4.44 (4.42); N, 30.86 (30.89); S, 11.77 (11.75).



Scheme-I: Synthesis of title compounds indolyl triazoles (IT1-8)

**3-(1H-Indol-3-ylmethyl)-5-thioxo-1,5-dihydro-4H-1,2,4-triazole-4-carbothioamide (IT4):** Yield: 65%; m.p.: 178-180 °C; FT-IR (KBr,  $\nu_{\max}$ , cm<sup>-1</sup>): 3488 (N-H), 1608 (C=N), 1582 (C=C), 1410 (C=S); <sup>1</sup>H NMR (DMSO-*d*<sub>6</sub>,  $\delta$  ppm): 3.80 (2H, s), 6.91-7.16 (2H, 6.99 (dd), 7.08 (dd)), 7.27-7.46 (2H, 7.34 (dd), 7.41 (tt)), 7.63 (1H, (dd)); <sup>13</sup>C NMR (DMSO,  $\delta$  ppm): 29.2 (1C, s), 110.5 (1C, s), 111.3 (1C, s), 118.7 (1C, s), 123.2 (1C, s), 127.3 (1C, s), 128.2 (1C, s), 128.4 (1C, s), 136.4 (1C, s), 150.9 (1C, s), 170.1 (1C, s), 182.8 (1C, s); MS (*m/z*, %): 289.06 (M<sup>+</sup>); Anal. calcd. (found) % for C<sub>12</sub>H<sub>11</sub>N<sub>5</sub>S<sub>2</sub>: C, 49.81 (49.83); H, 3.83 (3.86); N, 24.20 (24.22); S, 22.16 (22.14).

**4-(4-Chlorophenyl)-5-(1H-indol-3-ylmethyl)-2,4-dihydro-3H-1,2,4-triazole-3-thione (IT5):** Yield: 72%; m.p.: 198-200 °C; FT-IR (KBr,  $\nu_{\max}$ , cm<sup>-1</sup>): 3487 (N-H), 1598 (C=N), 1585 (C=C), 1415 (C=S), C-Cl (1107); <sup>1</sup>H NMR (DMSO-*d*<sub>6</sub>,  $\delta$  ppm): 3.82 (2H, s), 6.91-7.16 (2H, 6.99 (dd), 7.08 (dd)), 7.27-7.55 (6H, 7.34 (dd), 7.41 (tt), 7.45 (dd), 7.48 (dd)), 7.63 (1H, dd); <sup>13</sup>C NMR (DMSO,  $\delta$  ppm): 29.2 (1C, s), 110.5 (1C, s), 111.3 (1C, s), 118.7 (1C, s), 123.2 (1C, s), 125.9 (2C, s), 127.3 (1C, s), 128.2 (1C, s), 128.4 (1C, s), 128.9 (2C, s), 133.7 (1C, s), 136.4 (1C, s), 145.1 (1C, s), 150.9 (1C, s), 170.1 (1C, s); MS (*m/z*, %): 340.05 (M<sup>+</sup>); Anal. calcd. (found) % for C<sub>17</sub>H<sub>13</sub>N<sub>4</sub>SCl: C, 59.91 (59.94); H, 3.84 (3.83); Cl, 10.40 (10.42); N, 16.44 (16.47); S, 9.41 (9.43).

**4-(4-Bromophenyl)-5-(1H-indol-3-ylmethyl)-2,4-dihydro-3H-1,2,4-triazole-3-thione (IT6):** Yield: 70%; m.p.: 206-208 °C; FT-IR (KBr,  $\nu_{\max}$ , cm<sup>-1</sup>): 3485 (N-H), 1415 (C=S), 1600 (C=N), 1580 (C=C), C-Br (1093); <sup>1</sup>H NMR (DMSO-*d*<sub>6</sub>,  $\delta$  ppm): 3.82 (2H, s), 6.91-7.16 (2H, 6.99 (dd), 7.08 (dd)), 7.27-7.69 (7H, 7.34 (dd), 7.41 (tt), 7.44 (dd), 7.51 (dd), 7.63 (dd)); <sup>13</sup>C NMR (DMSO,  $\delta$  ppm): 29.2 (1C, s), 110.5 (1C, s), 111.3 (1C, s), 118.7 (1C, s), 122.3 (1C, s), 123.2 (1C, s), 127.3 (1C, s), 127.6 (2C, s), 128.2 (1C, s), 128.4 (1C, s), 131.7 (2C, s), 136.4 (1C, s), 145.1 (1C, s), 150.9 (1C, s), 170.1 (1C, s); MS (*m/z*, %):

385.03 (M<sup>+</sup>); Anal. calcd. (found) % for C<sub>17</sub>H<sub>13</sub>N<sub>4</sub>SBr: C, 53.02 (53.04); H, 3.40 (3.38); Br, 20.74 (20.76); N, 14.54 (14.57); S, 8.32 (8.30).

**5-(1H-Indol-3-ylmethyl)-4-(4-nitrophenyl)-2,4-dihydro-3H-1,2,4-triazole-3-thione (IT7):** Yield: 62%; m.p.: 183-185 °C; FT-IR (KBr,  $\nu_{\max}$ , cm<sup>-1</sup>): 3486 (N-H), 1596 (C=N), 1582 (C=C), 1410 (C=S), 1356 (C-NO<sub>2</sub>); <sup>1</sup>H NMR (DMSO-*d*<sub>6</sub>,  $\delta$  ppm): 3.82 (2H, s), 6.91-7.16 (2H, 6.99 (dd), 7.08 (dd)), 7.27-7.46 (2H, 7.34 (dd), 7.41 (tt)), 7.53-7.73 (5H, 7.59 (dd), 7.63 (dd), 7.67 (dd)); <sup>13</sup>C NMR (DMSO,  $\delta$  ppm): 29.2 (1C, s), 110.5 (1C, s), 111.3 (1C, s), 114.4 (2C, s), 117.7 (2C, s), 118.7 (1C, s), 123.2 (1C, s), 127.3 (1C, s), 128.2 (1C, s), 128.4 (1C, s), 136.4 (1C, s), 139.5 (1C, s), 145.1 (1C, s), 150.9 (1C, s), 170.1 (1C, s); MS (*m/z*, %): 351.07 (M<sup>+</sup>); Anal. calcd. (found) % for C<sub>17</sub>H<sub>13</sub>N<sub>5</sub>O<sub>2</sub>S: C, 58.11 (58.14); H, 3.73 (3.72); N, 19.93 (19.96); O, 9.11 (9.13); S, 9.13 (9.16).

**5-(1H-Indol-3-ylmethyl)-4-(4-methylphenyl)-2,4-dihydro-3H-1,2,4-triazole-3-thione (IT8):** Yield: 72%; m.p.: 191-193 °C; FT-IR (KBr,  $\nu_{\max}$ , cm<sup>-1</sup>): 3482 (N-H), 1407 (C=S), 1594 (C=N), 1578 (C=C), 3041 (C-H); <sup>1</sup>H NMR (DMSO-*d*<sub>6</sub>,  $\delta$  ppm): 2.22 (3H, s), 3.82 (2H, s), 6.91-7.21 (4H, 6.99 (dd), 7.08 (dd), 7.14 (dd)), 7.26-7.46 (4H, 7.32 (dd), 7.34 (dd), 7.41 (tt)), 7.63 (1H, (dd)); <sup>13</sup>C NMR (DMSO,  $\delta$  ppm): 21.3 (1C, s), 29.2 (1C, s), 110.5 (1C, s), 111.3 (1C, s), 112.0 (2C, s), 118.7 (1C, s), 123.2 (1C, s), 127.3 (1C, s), 128.2 (1C, s), 128.4 (1C, s), 129.6 (2C, s), 136.4 (1C, s), 141.5 (1C, s), 145.1 (1C, s), 150.9 (1C, s), 170.1 (1C, s); MS (*m/z*, %): 320.06 (M<sup>+</sup>); Anal. calcd. (found) % for C<sub>18</sub>H<sub>16</sub>N<sub>4</sub>S: C, 67.47 (67.49); H, 5.03 (5.02); N, 17.49 (17.51); S, 10.01 (10.04).

### In silico toxicity assessment

#### Prediction of activity for synthesized compounds (IT1-8):

The 2D molecular structures of the synthesized indolyl triazoles (IT1-8) sketched using MarvinSketch directly on the PASS

prediction website, which operates a JAVA applet [21]. By comparing the structure of each molecule with bioactive compounds in the PASS database, their biological activities were predicted. The PASS tool assesses the likelihood of activity versus inactivity (Pa-Pi ratio) at prediction thresholds of Pa > 30% and Pa > 70%. The predictions included a range of pharmacological actions and biological effects, emphasizing the potential antitubercular properties of the synthesized compounds.

**Bioactivity scores:** The bioactivity score of the synthesized compounds against key molecular targets such as receptors, enzymes and ion channels were calculated using the Molinspiration platform. Molecules that have a bioactivity score above 0.00 are probable to demonstrate substantial biological effects, whereas molecules with scores ranging from -0.50 to 0.00 are anticipated to have some level of activity. If the score is below -0.50, it is assumed that the molecule is not active [22].

**ProTox 3.0:** ProTox 3.0 integrates structural similarity, fragment analysis, common features and machine learning across a total of 61 models for predicting toxicity properties [23]. These properties encompass acute and organ toxicity, toxicological endpoints, molecular initiating events and metabolism. The 2D structures of synthesized compounds were input into ProTox 3.0 and predictions were obtained for each toxicity property.

### Biological activity

**Antitubercular activity:** The effectiveness of the synthesized indolyl triazoles (IT1-8) in treating tuberculosis was assessed using the microplate Alamar blue assay (MABA). The test used the *M. tuberculosis* H37RV strain as the infectious agent, with isonicotinic acid hydrazide (INH) acting as the control medication. To prepare for the assay, a clean 96-well plate was prepared, with sterile deionized water added to the outer wells to reduce medium evaporation. Every well was given 100  $\mu$ L of Middlebrook 7H9 (MB 7H9) broth and then the title compounds were serially diluted on the plate. The compounds' concentrations varied from 0.2 to 100  $\mu$ g/mL in the end. After a 5-day incubation period, the Alamar blue reagent was introduced into every well. The findings were analyzed according to the colour change: blue represented absence of bacterial growth, while pink signified bacterial growth [24].

**Antibacterial activity:** The effectiveness of compounds IT1-8 against a range of Gram-negative (*Escherichia coli*, *Pseudomonas aeruginosa*) and Gram-positive (*Staphylococcus epidermidis*, *Bacillus subtilis*) bacteria was evaluated through the agar cup plate method [25]. The method used ciprofloxacin as the reference standard. The growth medium used was Brain Heart Infusion (BHI) agar and bacterial suspensions were prepared to a 0.5 McFarland turbidity standard. The bacterial suspensions were evenly spread on the agar plates and a hollow tube was used to develop wells. Different amounts of the specified substances were added to the wells and then allowed to incubate. Measurements of the inhibition zones were taken after a 24 h incubation period. Minimum inhibitory concentration values were established by conducting serial dilutions, offering a comprehensive assessment of the antibacterial effectiveness of the synthesized compounds [25].

## RESULTS AND DISCUSSION

**Scheme-I** outlines the synthetic pathway utilized for synthesizing the indolyl triazoles (IT1-8). The process commenced with the reaction between indole acetic acid and hydrazine, yielding the hydrazide. Subsequently, the hydrazide underwent a reaction with CS<sub>2</sub> under basic conditions, leading to the formation of an indolyl oxadiazole thiol intermediate. This sequential process facilitated displacement and cyclization reactions, ultimately resulting in the generation of the intermediate. Following this, the intermediate underwent a displacement reaction with various hydrazine derivatives and aromatic amino reagents, yielding the final indolyl triazoles (IT1-8).

The purity of the synthesized compounds was confirmed using TLC, employing a mobile phase consisting of ethyl acetate, *n*-hexane and methanol. Moreover, unique peaks were detected in both IR and NMR spectra, indicating their structural integrity conclusively. Mass spectra analysis additionally confirmed the successful synthesis by verifying the existence of expected fragments of the molecular ion peak (M<sup>+</sup>).

Table-1 displays the PASS profiles, derived from a large training dataset containing 60,000 bioactive compounds with 4,500 unique mechanisms and activities. The likelihood of specific activities is indicated by the calculated probabilities (Pa and Pi). At first, it was anticipated that all the substances would show anti-tuberculosis and anti-mycobacterial effects with Pa values near 0.5 and none of the compounds were projected to have antibacterial abilities. However, the experimental results disagreed with these predictions, revealing significant antibacterial effects.

It is significant that the 2D molecular structure determines the prediction of activity spectra for compounds; hence, the accuracy of the computation is not certain to be 100% regarding bioactivity. Nevertheless, this computer-aided drug design tool is crucial in the optimization of lead or ligands, thereby improving the process of drug design and development while unveiling the novel molecular pathways. It also facilitates the identification of potential new leads through high-throughput screening of compound series. Thus, PASS predicted promising pharmacological potential for the synthesized indolyl triazole compounds (IT1-8) particularly in antitubercular and anticancer contexts.

Fig. 1 shows the anticipated bioactivity scores for all the synthesized compounds using Molinspiration. Compounds IT1 and IT2 are particularly impressive in terms of their bioactivity scores compared to other compounds. These results highlight the possibility of using compounds IT1 and IT2 as GPCR ligands and enzyme inhibitors. On the other hand, the remaining

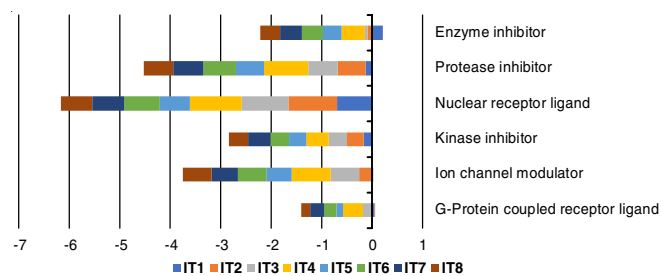


Fig. 1. Calculated bioactivity scores of synthesized compounds (IT1-8)

TABLE-1  
PASS PROFILE OF SYNTHESIZED COMPOUNDS (IT1-8)

Compd.	Pa	Pi	Activity	Compd.	Pa	Pi	Activity
<b>IT1</b>	0.603	0.038	Acute neurologic disorders	<b>IT5</b>	0.382	0.021	Antineoplastic
	0.443	0.021	Antituberculosic		0.355	0.071	Analgesic, non-opioid
	0.422	0.013	Antineoplastic		0.351	0.048	Antituberculosic
	0.381	0.044	Antimycobacterial		0.268	0.103	Antimycobacterial
<b>IT2</b>	0.510	0.033	Anticonvulsant	<b>IT6</b>	0.436	0.012	Antineoplastic
	0.371	0.024	Antineoplastic		0.429	0.024	Antituberculosic
	0.320	0.088	Autoimmune disorders		0.353	0.054	Antimycobacterial
	0.219	0.146	Antituberculosic		0.390	0.093	Antianginal
<b>IT3</b>	0.365	0.026	Antineoplastic	<b>IT7</b>	0.549	0.030	Antianginal
	0.369	0.110	Antianginal		0.493	0.013	Antituberculosic
	0.348	0.185	Acute neurologic disorders		0.432	0.011	Antineoplastic
	0.189	0.185	Antituberculosic		0.391	0.041	Antimycobacterial
<b>IT4</b>	0.393	0.018	Antineoplastic	<b>IT8</b>	0.456	0.055	Antianginal
	0.253	0.004	Antiacromegalic		0.388	0.019	Antineoplastic
	0.228	0.142	Antimycobacterial		0.379	0.038	Antituberculosic
	0.221	0.143	Antituberculosic		0.279	0.094	Antimycobacterial

substances show negative values suggesting the lower expected bioactivity. These findings highlight the complex nature of the physiological effects of drug combinations, indicating participation in several mechanisms and associations with different targets. The bioactivity scores obtained indicate a moderate interaction with all drug targets.

To assess potential oral toxicity risks associated with the synthesized indolyl triazoles (**IT1-8**), ProTox 3.0, a virtual lab for predicting toxicities of small molecules, was utilized. This tool evaluated various toxicological endpoints such as hepatotoxicity, carcinogenicity, immunotoxicity, mutagenicity and cytotoxicity, as outlined in Table-2. The *in silico* results obtained through ProTox 3.0 offer a comprehensive understanding of the toxicological effects associated with each compound. In terms of cytotoxicity, mutagenicity, immunotoxicity, carcinogenicity and hepatotoxicity, compound **IT5** is expected to demonstrate complete safety. Conversely, compound **IT6** is anticipated to be non-carcinogenic and non-cytotoxic; however, it exhibits active hepatotoxicity and mutagenicity. The remaining

compounds are characterized by moderate levels of toxicity.

The network chart generated by ProTox 3.0 visually represents the relationship between the selected compound and predicted activities, indicating whether the compound is active or inactive in terms of toxicity. Fig. 2 displays the toxicity network chart for synthesized compound **IT5**. In this chart, blue nodes represent compound **IT5**, while red nodes indicate predicted active toxicity and green nodes represent predicted inactive toxicity. This visualization offers a clear overview of the predicted toxicological profile of compound **IT5** based on ProTox 3.0 analysis.

Additionally, the toxicity chart from ProTox 3.0 provides a rapid overview of the confidence in positive toxicity predictions compared to the average of its class. This chart succinctly illustrates predicted toxicological endpoints for each compound displaying their relative positions in terms of toxicity compared to average class values. Fig. 3 presents the toxicity radar chart for compound **IT5**, providing insights into its predicted toxicity profile within the context of its chemical class.

TABLE-2  
ORAL TOXICITY REPORT OF INDOLYL TRIAZOLES (IT1-8)

Comp.	Target	Prediction	Probability	LD <sub>50</sub> (mg/kg)	Toxicity class	Comp.	Target	Prediction	Probability	LD <sub>50</sub> (mg/kg)	Toxicity class
<b>IT1</b>	Hepatotoxicity	Active	0.58	1200	4	<b>IT5</b>	Hepatotoxicity	Inactive	0.51	2500	5
	Carcinogenicity	Active	0.52				Carcinogenicity	Inactive	0.55		
	Immunotoxicity	Inactive	0.99				Immunotoxicity	Inactive	0.99		
	Mutagenicity	Inactive	0.55				Mutagenicity	Inactive	0.51		
	Cytotoxicity	Inactive	0.71				Cytotoxicity	Inactive	0.75		
<b>IT2</b>	Hepatotoxicity	Active	0.55	1500	4	<b>IT6</b>	Hepatotoxicity	Active	0.50	2500	5
	Carcinogenicity	Active	0.54				Carcinogenicity	Inactive	0.52		
	Immunotoxicity	Inactive	0.99				Immunotoxicity	Inactive	0.96		
	Mutagenicity	Inactive	0.56				Mutagenicity	Active	0.50		
	Cytotoxicity	Inactive	0.68				Cytotoxicity	Inactive	0.73		
<b>IT3</b>	Hepatotoxicity	Active	0.51	2000	4	<b>IT7</b>	Hepatotoxicity	Active	0.55	2500	5
	Carcinogenicity	Active	0.54				Carcinogenicity	Active	0.73		
	Immunotoxicity	Inactive	0.98				Immunotoxicity	Inactive	0.97		
	Mutagenicity	Active	0.50				Mutagenicity	Active	0.84		
	Cytotoxicity	Inactive	0.62				Cytotoxicity	Inactive	0.78		
<b>IT4</b>	Hepatotoxicity	Active	0.53	2000	4	<b>IT8</b>	Hepatotoxicity	Inactive	0.50	2500	5
	Carcinogenicity	Active	0.54				Carcinogenicity	Active	0.58		
	Immunotoxicity	Inactive	0.99				Immunotoxicity	Inactive	0.99		
	Mutagenicity	Active	0.52				Mutagenicity	Active	0.57		
	Cytotoxicity	Inactive	0.54				Cytotoxicity	Inactive	0.72		

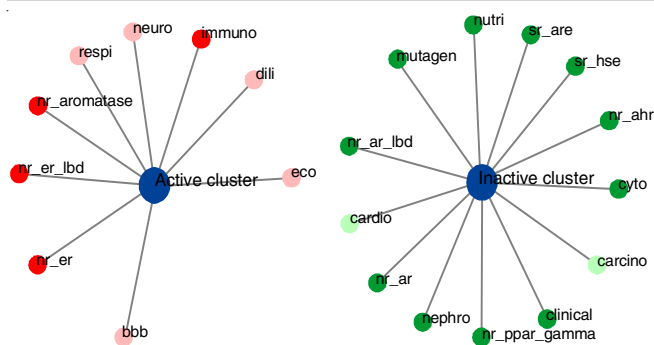


Fig. 2. Toxicity network chart of synthesized compound **IT5**

In addition to the toxicity network and radar charts, we examined the distribution of molecular weight and dose values in ProTox 3.0 to compare the input compound with the dataset compounds. The graph displays the molecular weight distribution, highlighting the value of the input compound in black

and the mean value of the dataset in red. The graph depicts the distribution of dose levels, with the input compound's value indicated in black and the average dataset value highlighted in red. These visualizations, depicted in Fig. 4, facilitate a clear comparison of the input compound's properties with those of the dataset, emphasizing key characteristics related to molecular weight and dose values.

**Antitubercular activity:** Table-3 shows that compounds **IT5** and **IT6**, with a halophenyl group at the 4th position of the 1,2,4-triazole ring, exhibited a significant activity at the concentrations of 25, 50 and 100  $\mu\text{g}/\text{mL}$ . The electron modulating abilities and lipophilicity enhancement from the halogen groups are likely reasons for the compounds' observed potency. The other compounds did not show significant activity at 25  $\mu\text{g}/\text{mL}$  or lower. Compounds **IT1** and **IT8**, which have electron donating substituents at the 4th position of the triazole ring, demonstrated activity at 50 and 100  $\mu\text{g}/\text{mL}$  concentrations. Substituents with isosteric or electron-attracting characteristics

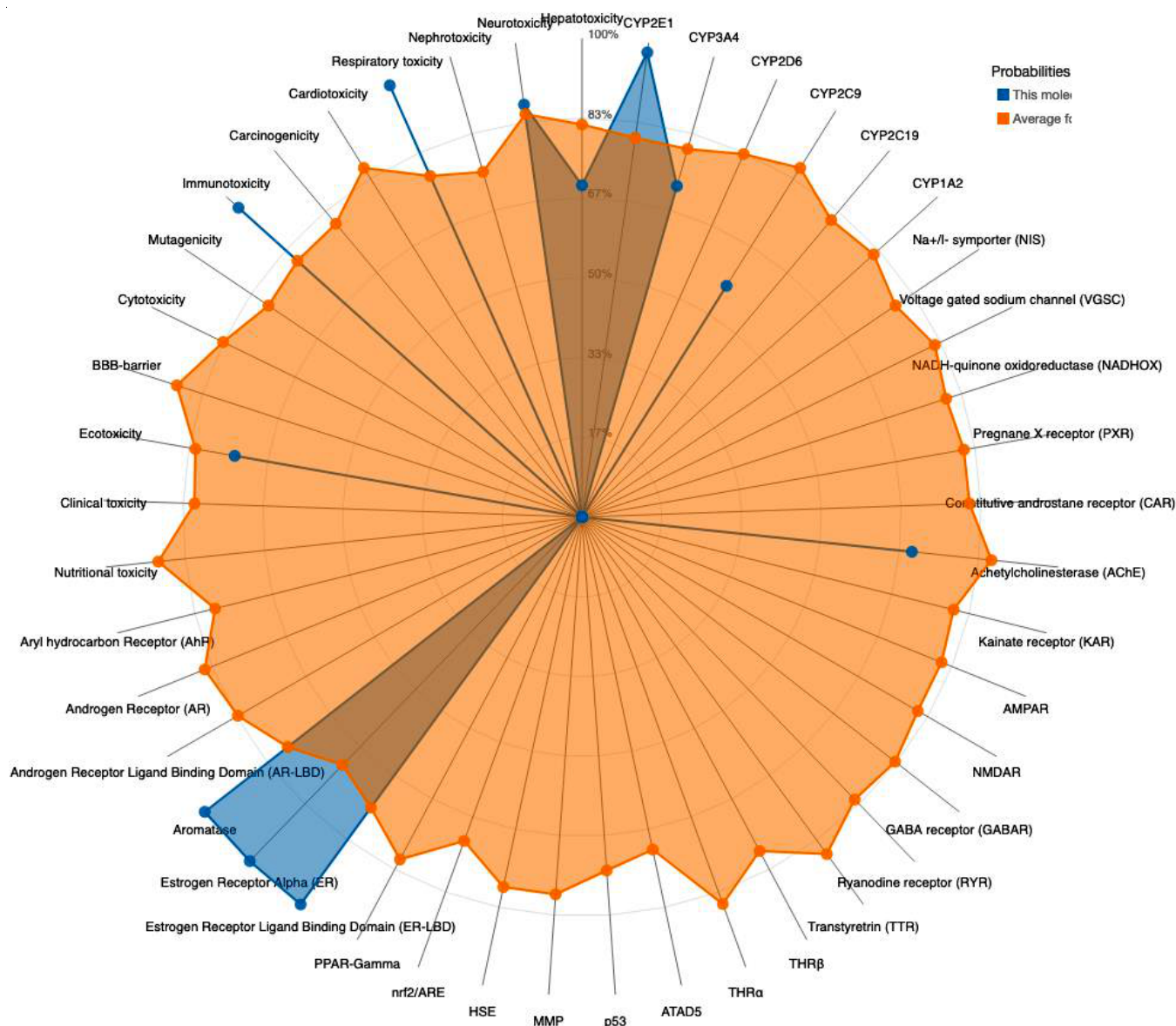


Fig. 3. Toxicity radar chart of synthesized compound **IT5**

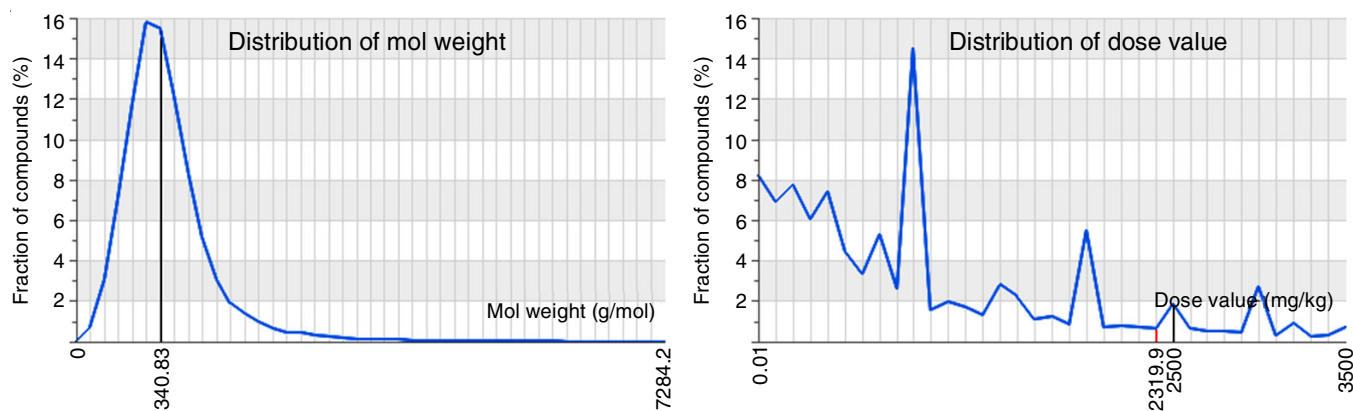


Fig. 4. Comparison of synthesized compound **IT5** properties with dataset characteristics

Compd.	Minimum inhibitory concentration		
	25 $\mu\text{g/mL}$	50 $\mu\text{g/mL}$	100 $\mu\text{g/mL}$
<b>IT1</b>	R	S	S
<b>IT2</b>	R	R	R
<b>IT3</b>	R	R	R
<b>IT4</b>	R	R	S
<b>IT5</b>	S	S	S
<b>IT6</b>	S	S	S
<b>IT7</b>	R	R	S
<b>IT8</b>	R	S	S
INH	S	S	S

at the same position in compounds **IT2**, **IT3**, **IT4** and **IT7** led to reduced activity. When compared to the standard drug isoniazid (INH), none of the synthesized compounds exhibited activity at concentrations below 25  $\mu\text{g/mL}$ .

Interestingly, isosteric compounds **IT2** and **IT3**, which contain polar carbamate and carbodiimide groups at the 4th position of the 1,2,4-triazole ring, were inactive at all tested concentrations. This inactivity is intriguing given that both groups are polar, electron modulators and hydrogen bond contributors, characteristics typically considered essential for antitubercular activity. Another isostere, Compound **IT4**, containing a thioamide group, exhibited activity at 100  $\mu\text{g/mL}$ .

Considerable disparities in the antitubercular activity were observed among the synthesized compounds featuring an aryl ring at the 4th position of 1,2,4-triazole ring across all concentrations. Compounds with an aryl ring featuring a chlorine or bromine at the *para*-position exhibited activity at all tested concentrations. However, replacing the halogen with a strong electron puller, such as a nitro functional group or an electron donor, like a methyl group, reduced activity. Compound **IT8**, which has a *para*-tolyl ring on triazole, exhibited activity at 50 and 100  $\mu\text{g/mL}$  but was inactive at 25  $\mu\text{g/mL}$ . In contrast, compound **IT7**, with a *para*-nitrophenyl ring, was inactive at 25 and 50  $\mu\text{g/mL}$  but showed activity at 100  $\mu\text{g/mL}$ . This diversity in activity highlights the significance of subtle structural disparities in shaping the antitubercular effectiveness of the title compounds, emphasizing the need for additional research to elucidate the structure-activity relationships governing their antitubercular properties.

**Antibacterial activity:** The antibacterial activity of all synthesized compounds (**IT1-8**) was evaluated using the agar cup-plate method, with ciprofloxacin used as the reference standard. Although *in silico* studies did not predict antibacterial effects, significant antibacterial activity was observed for all tested compounds at a dosage of 100  $\mu\text{g/mL}$  as shown in Fig. 5. Due to the presence of halogen atoms, compounds **IT5** and **IT6** exhibited the highest level of activity against the tested bacterial strains, which is consistent with the findings of the antitubercular evaluation. The significant antibacterial efficacy observed in all the synthesized compounds might be attributed to the presence of the indolyl ring attached to the triazole thione moiety. Likewise, the antibacterial properties of these compounds might have been influenced by the presence of substituted phenyl groups and isosteric carbamate groups. The structural features, particularly the halogenated phenyl rings and the presence of the indolyl and carbamate groups, play a crucial role in enhancing the antibacterial efficacy of these compounds.

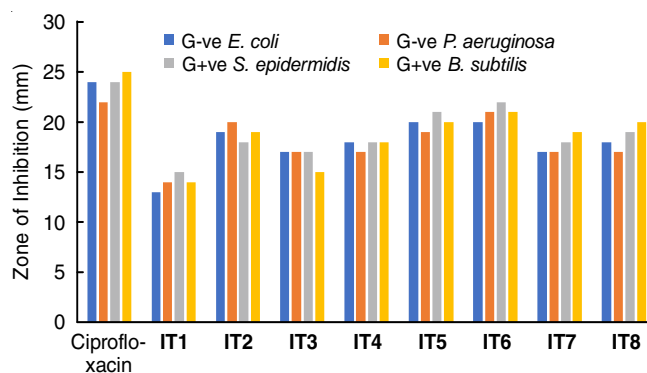


Fig. 5. Antibacterial activity of synthesized compounds **IT1-8**

Due to the halogen atoms, compounds **IT5** and **IT6** exhibited strong activity against the tested bacterial strains, which aligns with the findings of the antitubercular evaluation. The significant antibacterial efficacy found in all compounds can be attributed to the presence of the indolyl ring system linked to the triazole thione molecule. Similarly, the antibacterial characteristics of these compounds could have been affected by the presence of substituted phenyl groups and isosteric carbamate groups. The antibacterial activity of these compounds

is significantly enhanced by the structural components, particularly the halogenated phenyl rings as well as the presence of the indolyl and carbamate groups.

### Conclusion

The synthesis of indolyl-triazole hybrid molecules (**IT1-8**) has been successfully achieved, with their structures confirmed by advanced spectroscopic techniques. These compounds exhibit promising antimicrobial properties, particularly against bacterial strains, due to the structural features of halogenated phenyl rings and indolyl moieties. Computational analyses using PASS and Molinspiration predicted significant antitubercular and anticancer activities, identifying compounds **IT1** and **IT2** as potential GPCR ligands and enzyme inhibitors. However, the *in silico* predictions did not fully align with experimental antimicrobial results, underscoring the complexity of drug interactions and the limitations of computational tools alone. The toxicological assessments highlighted **IT5** as a compound with favourable safety profiles, while others demonstrated varying levels of toxicity. This research demonstrates the potential of indolyl-triazoles as effective antimicrobial agents and emphasizes the importance of integrating experimental and computational approaches in drug development. Further investigations into the structure-activity relationships is essential to optimize these compounds for the clinical applications.

### ACKNOWLEDGEMENTS

The authors express their gratitude for the material support received from Dr. M.G.R. Educational and Research Institute, K.B.H.S.S. Trust's Institute of Pharmacy, Seven Hills college of Pharmacy, Vignan Pharmacy College, MB School of Pharmaceutical Sciences, SV College of Pharmaceutical Sciences and Punjabi University. The authors conveyed their special thanks to Government Dental College and Research Institute, Bellary, for antitubercular evaluation studies. Finally, the authors extend their appreciation to the authorities of PASS, Molinspiration and ProTox 3.0 for generously providing the free softwares.

### CONFLICT OF INTEREST

The authors declare that there is no conflict of interests regarding the publication of this article.

### REFERENCES

1. S. Rehman, *J. Infect Public Health*, **16**, 611 (2023); <https://doi.org/10.1016/j.jiph.2023.02.021>
2. Antimicrobial Resistance Collaborators, *The Lancet*, **399**, 629 (2022); [https://doi.org/10.1016/S0140-6736\(21\)02724-0](https://doi.org/10.1016/S0140-6736(21)02724-0)
3. F. Prestinaci, P. Pezzotti and A. Pantosti, *Pathog. Glob. Health*, **109**, 309 (2015); <https://doi.org/10.1179/2047773215Y.0000000030>
4. K.W.K. Tang, B.C. Millar and J.E. Moore, *Br. J. Biomed. Sci.*, **80**, 11387 (2023); <https://doi.org/10.3389/bjbs.2023.11387>
5. O.B. Jonas, A. Irwin, F.C.J. Berthe, F.G. Le Gall and P.V. Marquez, Drug-Resistant Infections: A Threat to Our Economic Future: Final Report, HNP/Agriculture Global Antimicrobial Resistance Initiative Washington, D.C.: World Bank Group (2017); <http://documents.worldbank.org/curated/en/323311493396993758/final-report>
6. D. Vishwakarma, A. Gaidhane, S. Sahu and A.S. Rathod, *Cureus*, **15**, e50222 (2023); <https://doi.org/10.7759/cureus.50222>
7. S. Ajulo and B. Awosile, *PLoS One*, **19**, e0297921 (2024); <https://doi.org/10.1371/journal.pone.0297921>
8. M. Aatif, M.A. Raza, K. Javed, S.M. Nashre-Ul-Islam, M. Farhan and M.W. Alam, *Antibiotics*, **11**, 1750 (2022); <https://doi.org/10.3390/antibiotics11121750>
9. R. Aggarwal and G. Sumran, *Eur. J. Med. Chem.*, **205**, 112652 (2020); <https://doi.org/10.1016/j.ejmech.2020.112652>
10. H. Shirinzadeh, S. Süzen, N. Altanlar and A.D. Westwell, *Turkish J. Pharm. Sci.*, **15**, 291 (2018); <https://doi.org/10.4274/tjps.55707>
11. N. Teraiya, K. Agrawal, T.M. Patel, A. Patel, S. Patel, U. Shah, S. Shah, K. Rathod and K. Patel, *Curr. Drug Discov. Technol.*, **20**, 9 (2023); <https://doi.org/10.2174/1570163820666230505120553>
12. A. Dorababu, *RSC Med. Chem.*, **11**, 1335 (2020); <https://doi.org/10.1039/d0md00288g>
13. G.S. Reddy and M. Pal, *Curr. Med. Chem.*, **28**, 4531 (2021); <https://doi.org/10.2174/0929867327666200918144709>
14. B.S. Mathada and S.B. Somappa, *J. Mol. Struct.*, **1261**, 132808 (2022); <https://doi.org/10.1016/j.molstruc.2022.132808>
15. S.A. Al-Hussain, T.A. Farghaly, M.E.A. Zaki, H.G. Abdulwahab, N.T. Al-Qurashi and Z.A. Muhammad, *Bioorgan. Chem.*, **105**, 104330 (2020); <https://doi.org/10.1016/j.bioorg.2020.104330>
16. F. Pagniez, N. Lebouvier, Y.M. Na, I. Ourliac-Garnier, C. Picot, M. Le Borgne and P. Le Pape, *J. Enzyme Inhib. Med. Chem.*, **35**, 398 (2020); <https://doi.org/10.1080/14756366.2019.1705292>
17. H. Jahan, N.N. Siddiqui, S. Iqbal, F.Z. Basha, M.A. Khan, T. Aslam and M.I. Choudhary, *Life Sci.*, **291**, 120282 (2022); <https://doi.org/10.1016/j.lfs.2021.120282>
18. M.F. Youssef, M.S. Nafie, E.E. Salama, A.T.A. Boraei and E.M. Gad, *ACS Omega*, **7**, 45665 (2022); <https://doi.org/10.1021/acsomega.2c06531>
19. R. Reddyrajula, U. Etikyala, V. Manga and U.K. Dalimba, *Bioorg. Med. Chem.*, **98**, 117562 (2024); <https://doi.org/10.1016/j.bmc.2023.117562>
20. A.B. Danne, A.S. Choudhari, S. Chakraborty, D. Sarkar, V.M. Khedkar and B.B. Shingate, *Medchemcomm*, **9**, 1114 (2018); <https://doi.org/10.1039/c8md00055g>
21. D.A. Filimonov, A.A. Lagunin, T.A. Glorizova, D.S. Druzhilovskii, A.V. Rudik, P.V. Pogodin and V.V. Porokov, *Chem. Heterocycl. Compd.*, **50**, 444 (2014); <https://doi.org/10.1007/s10593-014-1496-1>
22. A. Ayar, M. Aksahin, S. Mesci, B. Yazgan, M. Gül and T. Yildirim, *Curr. Computeraided Drug Des.*, **18**, 52 (2022); <https://doi.org/10.2174/1573409917666210223105722>
23. P. Banerjee, E. Kemmler, M. Dunkel and R. Preissner, *Nucleic Acids Res.*, **52**, W513 (2024); <https://doi.org/10.1093/nar/gkac303>
24. S.G. Franzblau, R.S. Witzig, J.C. McLaughlin, P. Torres, G. Madico, A. Hernandez, M.T. Degnan, M.B. Cook, V.K. Quenzer, R.M. Ferguson and R.H. Gilman, *J. Clin. Microbiol.*, **36**, 362 (1998); <https://doi.org/10.1128/JCM.36.2.362-366.1998>
25. CLSI, M100 Performance Standards for Antimicrobial Susceptibility Testing, CLSI; Wayne, PA, USA, edn. 29 (2019).